

Weak ferromagnetism and possible non-Fermi-liquid behavior in the itinerant electronic material Co_3SnC

Bosen Wang,^{1,2,3,*} Yoshiya Uwatoko,³ Jinguang Cheng^{1,2} and Yuping Sun^{5,4}

¹Beijing National Laboratory for Condensed Matter Physics and Institute of Physics, Chinese Academy of Sciences, Beijing 100190, China

²Songshan Lake Materials Laboratory, Dongguan, Guangdong 523808, China

³Institute for Solid State Physics, University of Tokyo, Kashiwanoha 5-1-5, Kashiwa, Chiba 277-8581, Japan

⁴Key Laboratory of Materials Physics, Institute of Solid State Physics, Chinese Academy of Sciences, Hefei 230031, People's Republic of China

⁵High Magnetic Field Laboratory, Chinese Academy of Sciences, Hefei 230031, People's Republic of China



(Received 8 June 2019; revised 29 July 2020; accepted 29 July 2020; published 28 August 2020)

We report the observation of weak ferromagnetism and possible non-Fermi-liquid behavior in itinerant electronic material Co_3SnC via magnetic properties, electrical transport, and specific heat under various magnetic fields. The analysis of magnetic properties suggests that Co_3SnC undergoes a noncollinear itinerant ferromagnetic-paramagnetic phase transition around 3.6 K. With this transition, non-Fermi-liquid (NFL) behavior appears at low temperature covering a wide temperature range. The features of NFL are revealed by the power-law temperature dependence of resistivity and also proved by the $-T\log T$ dependence upturn in specific heat and the $T^{4/3}$ dependence of inverse susceptibility. With increasing the fields, the temperature coefficient of the T^2 term in the resistivity data shows a $(H - H_c)^{-0.5}$ divergence approaching the H_c and reduces monotonously with increasing the field further, apart from the usual $1/(H - H_c)$ dependence with the whole Fermi surface under the singular scattering. The exponent n in the temperature dependence of resistivity shows an increase from $n = 1.0$ to 2.0 with increasing the field as the evidence for the field-induced crossover from NFL to FL behavior; it is thought that field dependence of magnetic ground states should be responsible for this crossover; the relative mass enhancement factor $\lambda(H)/\lambda(0)$ reduces monotonically to nearly 60% at 9.0 T, indicating the gradual suppression of magnetic fluctuations and electron-electron scattering. Our results indicate that Co_3SnC is a candidate for exploring itinerant quantum materials.

DOI: [10.1103/PhysRevB.102.085153](https://doi.org/10.1103/PhysRevB.102.085153)

I. INTRODUCTION

In Fermi-liquid theory, the quasiparticle (QP) approximation and the generalized Boltzmann equation can describe the collective behaviors of strongly correlated multielectron systems [1]. For magnetic materials, strong magnetic correlations usually induce large changes in the QP-QP interactions, which makes the QPs behave abnormally [1,2]. In particular, approaching the magnetic quantum critical point (QCP), various pronounced deviations from the Landau Fermi liquid (FL) frequently appear [3,4], e.g., non-Fermi liquid (NFL) and strong enhancement of the QP-QP interaction. On these issues, many correlated electronic materials including heavy fermion (HF) systems which have been studied where magnetic orders are tuned by strongly strengthening the hybridizations of the $4f$ and conduction electrons and/or magnetic correlations via the external parameters [4,5]. These studies are helpful to reveal the intrinsic characteristics of the competing magnetic orders and QCPs. After several decades' explorations, many candidates have been found but the universal model is absent for the understanding of NFL behavior [3–9]. Most studies focus on the localized antiferromagnetic (AFM) orders, not itinerant

ferromagnetism although the QP-QP scattering involved with the localized and itinerant magnetism may have a different physical origin. The lack of studies makes the study on the itinerant ferromagnetism attractive. For example, the ZrZn_2 and $\text{Sc}_{3.1}\text{In}$ have been explored to show peculiar itinerant ferromagnetic (FM) QCPs by electronic substitutions and/or physical pressure [10,11] while the Sc-doped TiAu exhibits AFM QCPs [12], but different critical scaling behaviors were proposed. Thus, it is imperative to explore more itinerant electronic materials combined with theoretical calculations.

Cobalt-containing materials are such alternatives to explore exotic QCPs owing to the various spin states of cobalt ions and their strong response to the external stimuli [13]. Especially for those materials with both localized and itinerant electrons, the varieties of magnetic transition and phase diagram are more interesting. Metallic perovskite M_3MX (M is transition metals; M' is the main group elements; X is C, N) is such an example and has been paid considerable attention because of its diversified crystal structures and magnetic phase transitions [14,15]. Various functionalities have been discovered closely associated with these structural/magnetic phases [14,16–21]. However, the intrinsic magnetic interaction in M_3MX is controversial although various classical models were proposed [14,22–24]. One possible reason for the absence of the universal theoretical model is that the present system is not limited to the simple localized and/or

*Correspondent author: bswang@iphy.ac.cn

itinerant interactions [22,24]. Some reports have argued that these materials are close to the edge of the localized and itinerant ferromagnetism and thus can be seen as good targets to study the crossover between them [15,25]. Based on the Stoner itinerant ferromagnetic model, theoretical calculations predicated the universal conditions for the stabilizations of magnetic ground states for M_3MX [25,26]: The itinerant FM state is stable if satisfying the criterion $N(E_F)I > 1$ where $N(E_F)$ and I represent the density of states at the Fermi level E_F and the exchange integral of magnetic interaction, respectively. Actually, the magnetic properties of M_3MX ($M' = \text{Ga, Sn, etc.}$) have been widely studied via chemical doping although the magnetic structures are still unknown [14,27,28]. Some features have been also claimed for Co_3SnC such as the enlarged $N(E_F)$ value and Seebeck coefficient as well as relative weak exchange interaction [19,25]. Besides, Co_3SnC was reported to exhibit a FM-PM phase transition and physical properties strongly depend on the chemical compositions and experiment conditions [17,29], which, combined with the previous investigations, implies that the magnetic ground state of Co_3SnC could be unstable and thus abnormal quantum behaviors are expected by tuning nonthermodynamic parameters.

High pressure is a useful method to explore new materials by changing crystal structure and electronic structure. For the unstable phase, the quality of a sample is an important parameter and can be improved by high-pressure annealing. Many metastable phases can be stabilized after the annealing under high pressure/temperature, which may derive exotic physical phenomena [30,31]. In this sense, more explorations concerning the Co_3SnC would be valuable to uncover the enigmatic phase transition since the present studies are limited and not enough to figure out intrinsic physical properties. In this work, we report the magnetic susceptibility, electrical transport, and specific heat of Co_3SnC under magnetic fields up to 9.0 T. NFL behavior is revealed in the power-law temperature dependence of resistivity, together with the $-T \log T$ dependence in specific heat and the $T^{4/3}$ dependence in inverse susceptibility. Under magnetic field, the exponent n increases from $n = 1.0$ to 2.0 as evidence for the crossover from NFL to FL behavior. Our results suggest that Co_3SnC is a candidate for itinerant FM materials.

II. EXPERIMENTAL METHODS

Co_3SnC polycrystalline was prepared by reacting tin (5N), graphite (3N), and cobalt (5N). The first step is to prepare the polycrystalline sample at ambient pressure: The starting materials were mixed, sealed in quartz tubes under 0.5 atm of argon gas, and then annealed at 1073–1273 K for 10 days; after quenching to room temperature, the products were pulverized, mixed, pressed, and annealed at 1123 K for 1 week. During the process, the 5%–10% excess graphite was added to make up the carbon loss during the preparation. The second step is the annealing of a single-phase polycrystalline sample under high pressure and high temperature: The synthesized bulk Co_3SnC polycrystalline was pulverized by using a platinum tube and then treated at 4.0 GPa and 1223 K for 35 min. We note that the sample becomes hard and gray-black after high-pressure annealing. For comparisons, x-ray diffraction (XRD)

was performed at 300 K by x-ray diffractometer with $\text{Cu } K\alpha$ radiation ($\lambda = 0.15406 \text{ nm}$) for high-pressure annealed (S1#) and the as-synthesized Co_3SnC samples (S2#), respectively. The Rietveld refinement of XRD patterns is performed and the diffraction peaks are indexed to a cubic phase [space group: $Pm-3m$ (221); Co, 3c; Sn, 1b; C, 1a] (see Fig. S1 in the Supplemental Material [32]). Lattice parameters are $a = 0.3799(4)$ (S1#) and $0.3803(6)$ nm (S2#), which are close to those of the reports and theoretical simulations [19,25]. The Co/Sn ratio is also indicated by using energy dispersive x-ray analysis (EDX) [3.223(4)] and the Rietveld refinements [3.364(2)], which suggests the 5%–10% excessive Co atomic occupation in the Sn 1b site, which introduces the complicated interactions between the corner Co and the face-centered Co except for the 180 °C and the 90 °C Co-C-Co ones [22,33].

Electrical transport $\rho(T)$, heat capacity $C_p(T)$, and Seebeck coefficient $S(T)$ were measured on the Quantum Design physical property measurement system ($0 \leq H \leq 9.0 \text{ T}$, $1.8 \leq T \leq 400 \text{ K}$). Magnetic properties were measured on the Quantum Design superconducting quantum interference device ($0 \leq H \leq 9.0 \text{ T}$, $1.8 \leq T \leq 400 \text{ K}$). The sample for magnetic measurements can be considered as the ellipsoids and the applied field is basically parallel to its longest semi-axis. As a result, a uniform magnetic field exists throughout the sample and sharp demagnetizing fields are reduced. The standard four-probe technique was adapted to measure electrical transport and Seebeck coefficient.

III. RESULTS AND DISCUSSION

Figure 1(a) shows the temperature dependence of magnetic susceptibility $\chi(T) (= M/H)$ for Co_3SnC (S1#, S2#) at a magnetic field of 0.10 T. On cooling from 300 K, the M/H increases gradually and shows a saturated trend at lower temperature, which is usually accompanied by magnetic phase transition. For clarity, temperature dependence of the derivative $d(M/H)/dT$ and isothermal magnetization $M(H)$ curve are also examined. As shown in the inset of Fig. 1(a), a broad peak is found at $\sim 3.64 \text{ K}$ in the temperature dependence of $d(M/H)/dT$ at 0.10 T, which indicates the appearance of magnetic phase transition [14]. The $M(H)$ curves at 2 K are measured under zero-field-cooled processes in Fig. 1(b) for S1# and S2#, respectively. It is found that the magnetization increases quickly with increasing the field and shows a slope change around 1.50 T, but does not saturate with further increasing the fields up to 5.0 T. There is no magnetic hysteresis at lower fields as an indication of soft magnetism. Usually, the slope change can reflect the rotation of ferromagnetic domains under magnetic field for FM materials and the unsaturated magnetizations up to 5.0 T are the common features of the noncollinear ferromagnetism and/or the coexistence of AFM and FM interaction [14,19]. It is certain that the magnetic ground state of Co_3SnC should be FM. However, it is difficult to identify its detailed magnetic order and further neutron diffraction experiments are required. Besides, a slightly difference is found in both $\chi(T)$ and $M(H)$ curves for S1# and S2#, which is consistent with the contraction of lattice parameters after high-pressure annealing. For a stable FM phase, the linear extrapolation of Arrott plots (M^2 vs H/M) to $H = 0$ for $T < T_c$ gives the spontaneous magnetization M_s , which

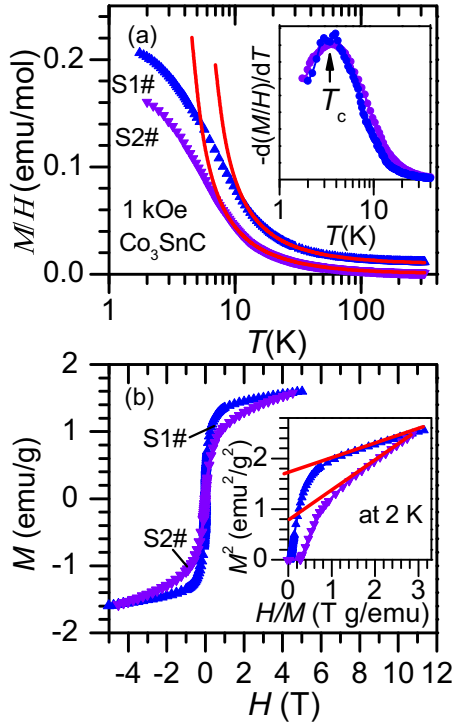


FIG. 1. (a) Temperature dependence of M/H at a magnetic field of 0.10 T for Co_3SnC (S1#, S2#) and the solid line represents the Curie-Weiss fitting. The inset shows the temperature dependence of $-d(M/H)/dT$; the arrow indicates the magnet transition temperature T_c . (b) Isothermal magnetization curves $M(H)$ at 2 K for S1# and S2#, respectively. The inset shows the Arrot plot of the M^2 vs H/M ; the red lines are linear fitting results of high-field data.

is evidence for the ferromagneticlike ground state [34]. For S1# and S2#, M_s is given from the linear extension as in the inset of Fig. 1(b). The values are 1.317(5) and 0.890(1) emu/g and nearly zero above T_c , which indicates weak ferromagnetism. The results also qualitatively explain the magnetic ground state, although it may involve noncollinear magnetic interaction.

To get more information, the temperature dependence of susceptibility was analyzed by the Curie-Weiss (CW) law $\chi(T) = \chi_0 + 0.37488\mu_{\text{eff}}/(T - \theta_c)$, where the characteristic parameters χ_0 , μ_{eff} , and θ_c represent the Pauli paramagnetic susceptibility, the effective moment, and the Curie-Weiss temperature, respectively. We note that the χ_0 value is about 9.47×10^{-3} , 1.65×10^{-3} emu/mol Oe; the μ_{eff} value $\sim 1.053(2)$, $0.951(3)$ $\mu_B/\text{Co f.u.}$; the θ_c value $\sim 4.688(6)$, $3.163(5)$ K for S1# and S2#, respectively. The μ_{eff} is nearly half the typical value of $2-4 \mu_B/\text{Co}$ for the localized magnetic moments. In Fig. 1(b), the maximal magnetizations [$M_s(5.0 \text{ T})$] are 0.0293(2) $\mu_B/\text{Co f.u.}$ and 0.0289(4) $\mu_B/\text{Co f.u.}$ for S1# and S2#, respectively. Thus, we can get the ratio $M_s(5.0 \text{ T})/\mu_{\text{eff}}$, which is usually used as the measure of itinerant degree of electron, of about 0.028(2) and 0.030(5) for S1# and S2#, respectively. These results suggest the weak itinerant ferromagnetism of Co_3SnC [13,19,22,33].

Temperature dependence of electrical resistivity $\rho(T)$ was compared for S1# and S2# in Fig. 2(a). They both exhibit metallic behavior but the temperature dependence of $\rho(T)$

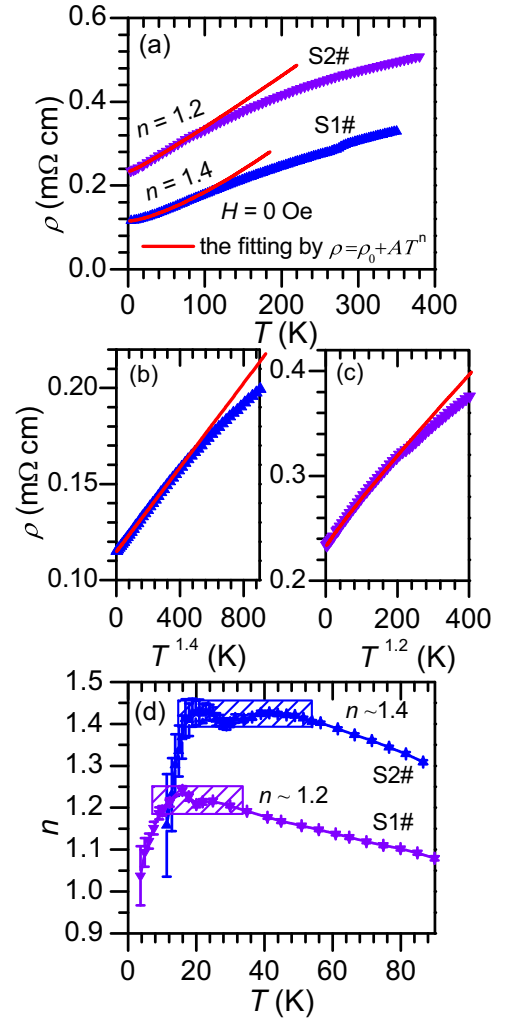


FIG. 2. (a) Electrical resistivity $\rho(T)$ and its analysis by the empirical formula $\rho = \rho_0 + AT^n$ with the residual resistivity ρ_0 , the temperature coefficient A , and the exponent n . (b) The plot of $\Delta\rho(T)$ vs $T^{1.4}$ for S1#; (c) the plot of $\Delta\rho(T)$ vs T^2 for S2#; the lines are the linear fitting results. (d) Temperature dependence of the $n(T_{\text{FL}})$ with different temperature ranges for $1.8 \text{ K} \leq T \leq T_{\text{FL}}$. The n value is $\sim 1.403(2)$ for S1# and $\sim 1.196(4)$ for S2#.

cause the usual Fermi-liquid behavior to deviate below 60 K. In detail, $\rho(T)$ was analyzed further by the formula $\rho = \rho_0 + AT^n$ with the residual resistivity ρ_0 , the temperature coefficient A , and the exponent n , respectively. We note that the n value strongly relies on the selection of temperature ranges sensitively. For accuracy, we selected the fixed temperature ranges of $1.8 \text{ K} \leq T \leq T_{\text{FL}}$ (the characteristic temperature), and got the exponent $n(T_{\text{FL}})$ with the fixed T_{FL} . For the best fitting, the value of $n(T_{\text{FL}})$ does not vary much and has a high degree of confidence, as indicated by the box in Fig. 2(d). The n is $\sim 1.403(2)$ for S1# and $\sim 1.196(4)$ for S2# (see Figs. 2(b) and 2(c), and Fig. S2 in the Supplemental Material [32]), which indicates clear NFL behavior [3,4]. Usually, it is well known that some nonintrinsic factors may induce similar behavior in dirty polycrystalline material. For example, lattice disorders and atomic vacancies may mask the electron-electron scatterings, but this scenario can be excluded

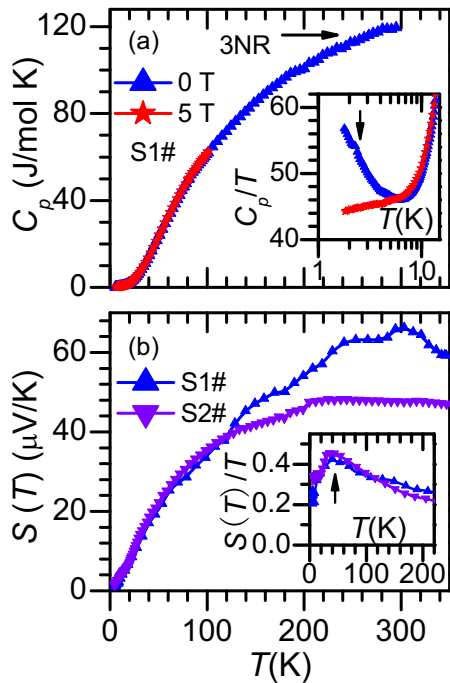


FIG. 3. (a) Specific heat $C_p(T)$ at 0 and 5 T for Co_3SnC (S1#); the inset shows the enlargement of the $C_p(T)/T$ vs T . (b) Temperature dependence of Seebeck coefficient $S(T)$ and temperature dependence of the $S(T)/T$ in the inset; the arrow indicates the peak of the $S(T)/T$ around 40 K.

by combining with field dependence of physical properties in the following texts.

In Fig. 3(a), the temperature-dependent specific heat $C_p(T)$ is shown for S1# and it increases monotonically on warming and approaches $\sim 3NR$ above 300 K; below 10 K, the $C_p(T)/T$ shows an abnormal upturn to the lowest temperature with a $-T\log T$ dependence as in the inset of Fig. 3(a) [2–4]; this upturn is gradually suppressed with increasing the fields up to 5.0 T, which is a feature of NFL behavior [3]. In addition, a small peak near 2.35 K can be found in the plot of $C_p(T)/T$ vs T at zero field, which is close to the T_c from the $d(MH)/dT$ at 10 Oe in Figs. 1(a) and S3 [32]. In Fig. 3(b), the temperature dependence of the Seebeck coefficient $S(T)$ is compared for S1# and S2#, respectively. $S(T)$ shows positive temperature dependence and trend to constants above 200 K. In the inset, the $S(T)/T$ shows a peak near 40 K; a positive Seebeck coefficient may manifest that hole-type carriers are dominant in the electronic bands of Co_3SnC . We note that its room-temperature magnitude is $65 \mu\text{V/K}$ for S1# and $48 \mu\text{V/K}$ for S2#, which are larger compared with other Co-based materials [19,27]. At last, we conclude that Co_3SnC shows weak itinerant ferromagnetism and unusual NFL behavior.

To study NFL behavior, magnetic field is a useful tool. In Figs. 4(a), 4(b), and 5(a), field-dependent $\rho(T)$ is measured for S1# under various fields up to 9.0 T. Similar to the analysis at zero field, both ρ_0 and n are estimated and the low- T part of $\Delta\rho = [\rho(T) - \rho_0]$ is presented in Figs. 4(a), 4(b), and 5(a). Field dependence of the parameters ρ_0 , A , and n is compared in Figs. 5(c)–5(e). It is found that the n

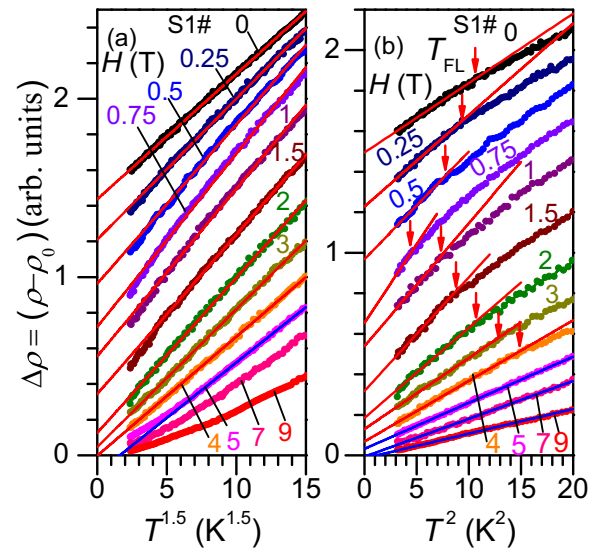


FIG. 4. Temperature dependence of $\rho(T)$ under various fields up to 9 T for Co_3SnC (S1#). The values of ρ_0 and the exponent n are estimated first and temperature dependence of the $\Delta\rho(T)$ [defined as $\rho(T) - \rho_0$] is obtained: (a) the plot of $\Delta\rho(T)$ vs $T^{1.5}$ for $n = 1.5$; (b) the plot of $\Delta\rho(T)$ vs T^2 for $n = 2$. For comparison, the $\Delta\rho(T)$ was translated at equal intervals; the characteristic temperature T_{FL} is defined as the deviation temperature from T^2 behavior and is marked by arrows in 2(b).

value decreases and reaches a minimum $\sim 1.103(5)$ around 0.75 T, and then increases up to $\sim 2.016(4)$ at 9.0 T, which suggests field-induced crossover from NFL to FL behavior [2,3]. For clarity, both the plot of $\Delta\rho$ vs $T^{1.5}$ and the plot

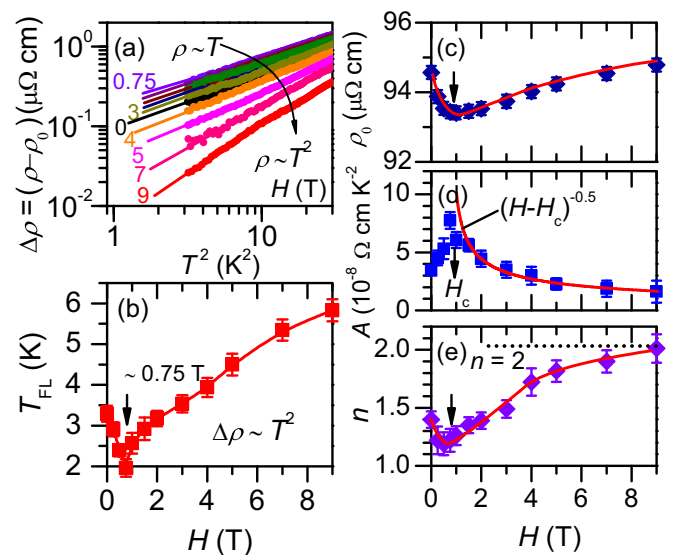


FIG. 5. (a) The plot of $\Delta\rho(T)$ vs T^2 in a log-log scale; the arrow shows the crossover from T to T^2 dependence. (b) Field dependence of the T_{FL} ; the arrow shows the critical field of 0.75 T. Field dependence of all the parameters: (c) ρ_0 ; (d) A and the exponential fitting results by the $(H - H_c)^{-0.5}$ (the red solid line); (e) n ; the arrows in (c), (e) indicate the change tendency and are guides to the eye. The dashed line represents $n = 2$.

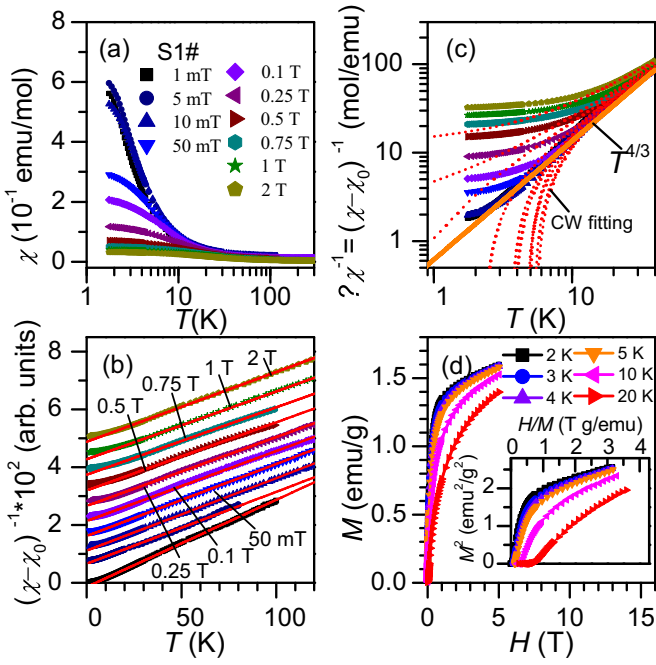


FIG. 6. (a) Temperature dependence of $\chi(T)(= M/H)$ under various fields up to 2.0 T for Co_3SnC (S1#). (b) Temperature dependence of $\Delta\chi^{-1} = (\chi - \chi_0)^{-1}$ and the red solid lines are the CW fitting results which is also translated at equal intervals. (c) The enlargement of low-temperature $\Delta\chi^{-1}(T)$ and the CW fitting results. The orange line represents the $T^{4/3}$ dependence. (d) $M(H)$ curves at 2, 3, 4, 5, 10, and 20 K for S1#; the inset shows the Arrot plot.

of $\Delta\rho$ vs T^2 are examined in Figs. 4(a) and 4(b). We find that the $\Delta\rho$ data show $T^{1.5}$ dependence for $H \leq 4.0$ T and clear departure from the linearity appears with further increasing the fields up to 9.0 T, which may manifest different scattering processes. In Fig. 4(b), the $\Delta\rho$ data show a linear temperature dependence below the T_{FL} , which reduces from 3.29 K at 0 T to 1.96 K for 0.75 T, and then enhances up to 5.83 K at 9.0 T [Fig. 5(b)]. This behavior reminds us of the feature and appearance of AFM QCPs [3,12,35], but rarely exists in itinerant FM materials because FM interactions are usually enhanced under magnetic fields [4–6].

Furthermore, as shown in Fig. 5(a), the log-log plots of $\Delta\rho$ vs T^2 clearly proved the crossover from NFL to FL behavior with increasing the field [e.g., $n \sim 1.403(2)$ to $\sim 1.103(5)$ at 0.75 T, then to $\sim 2.034(3)$ at 9.0 T]. The field dependence of $A(H)$ is plotted in Fig. 5(d), which is an important measure for the QP-QP scattering across the QCP regions. We find that it becomes maximum near the critical field H_c , and then decreases monotonically with further increasing the field. The further analysis suggests that field dependence of the $A(H)$ shows $(H - H_c)^{-0.5}$ divergences near H_c , which is different from the $1/(H - H_c)$ behavior where the whole Fermi surface is under singular scattering [3,4]. Anyway, these results elucidate that FL behavior is recovered at 9.0 T in the ground state of Co_3SnC . Finally, we summarized several features: (i) the inconsistent values of the Curie temperature T_c and the T_{FL} at lower fields; (ii) the ρ_0 and the T_{FL} reach the minimum at H_c . Whether NFL behavior and the crossover correlate with FM instability is unclear.

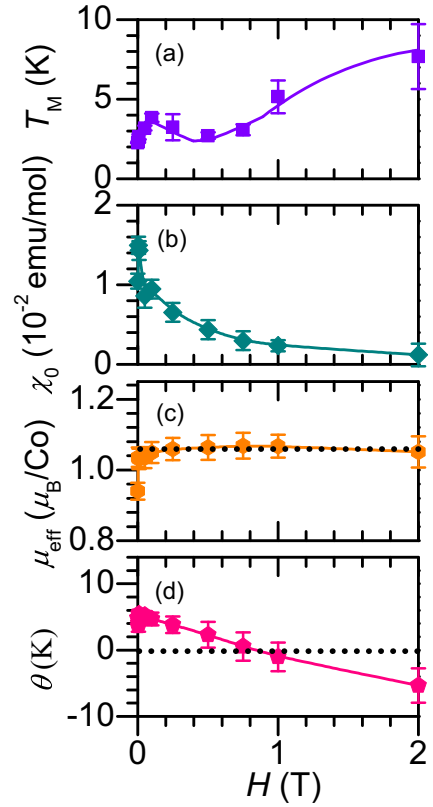


FIG. 7. Field dependence of the parameters: (a) the T_M ; (b) the χ_0 ; (c) the μ_{eff} ; (d) the θ_c . The solid lines indicate the change tendency and guides to the eye.

Temperature dependence of susceptibility $\chi(T)(= M/H)$ was measured for S1# with the fields up to 2.0 T as shown in Fig. 6(a) and the characteristic temperature T_M is defined as the peak temperature of $d(M/H)/dT$ in Figs. 1(a) and Fig. S3 [32]. It is mainly used to describe the magnetic properties closely related to electrical transport. However, the $d(M/H)/dT$ broadens largely with increasing the fields, which may indicate magnetic instabilities and the competition of various magnetic orders. For clarity, the T_M is determined from $d(M/H)/dT$ and the half width as the error as listed in Fig. S3 [32]. It is found that the value of T_M does not shows nonmonotonic increases with a minimum near the critical field and then increases monotonically. This origin of nonmonotonic change is unclear and may involve the competition of different magnetic interactions with increasing the fields [11]. In Fig. 6(b), by using the same methods as in Fig. 1(a), the temperature dependence of inverse susceptibility $\Delta\chi^{-1}(T) = (\chi - \chi_0)^{-1}$ was analyzed and the red solid lines represent the fitting results which are translated at equal intervals for clarity.

Field dependence of the parameters T_M , χ_0 , μ_{eff} , and θ_c are shown in Figs. 7(a)–7(d). The μ_{eff} is nearly field independent except for the quick increase at lower fields; this increase can be usually attributed to the field-induced ferromagnetic domain reversal; the θ_c decreases linearly with increasing the fields after an initial enhancement at lower fields. In the itinerant scenario, the Curie-Weiss behavior mainly arises from the temperature-dependent magnetic fluctuations; thus

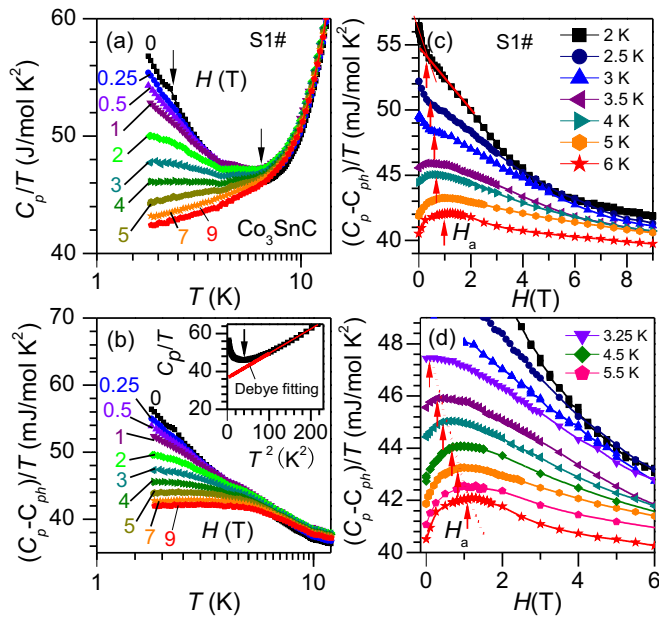


FIG. 8. (a) Temperature dependence of $C_p(T)/T$ vs $\log T$ under various fields up to 9.0 T for Co_3SnC (S1#). (b) The plot of $(C_p - C_{\text{ph}})/T$ vs $\log T$. Inset shows the plots of C_p/T vs T^2 and the linear fitting results. (c,d) Field dependence of the $(C_p - C_{\text{ph}})/T$ at various temperatures (2–6 K). For 2, 2.5, 3 K, the H_a value is defined as the intersections of two straight lines. For 3.25, 3.5–6 K, the H_a value is marked by the peak in the field dependence of the $(C_p - C_{\text{ph}})/T$. The dashed line shows its tendency.

the slight increases in the θ_c give rise to spin fluctuations from magnetic disorders at lower fields [4, 11]. With further increasing the field, the sign of θ_c changes its sign from positive to negative at P_c , which suggests that the dominant magnetic interaction may change with increasing the field. As plotted in Fig. 6(c), low- T $\Delta\chi^{-1}(T)$ changes gradually from $T^{4/3}$ dependence to a saturated trend at higher fields, which is a common feature of NFL behavior [1, 2]. As in Fig. 6(d), $M(H)$ curves are shown for selected temperatures and Arrot plots of M^2 vs H/M are in the inset for Co_3SnC (S1#). The $M(H)$ curve is unsaturated up to the highest field even above the Curie temperature determined from the $M(T)$. Accordingly, the Curie temperature determined by the M^2 vs H/M plot is slightly higher than those from $d(M/H)dT$ vs T , which suggests that the mean-field scaling theory is not suitable. Similar inconsistent features were reported in other itinerant FM materials and magnetic fluctuations under higher field should be responsible [11, 36].

Specific heat is a good tool to investigate bulk and intrinsic physical properties of materials. As shown in Fig. 8(a), temperature dependence of $C_p(T)/T$ is plotted for Co_3SnC (S1#) under fields. We find that logarithmic temperature dependence of $C_p(T)/T$ exhibits an upturn below ~ 10 K and this upturn is gradually suppressed for the field $H > 4.0$ T, consistent with the field-induced crossover from NFL to FL behavior [2]. Generally, the magnetic contribution $C_M(T)$ is $T^{3/2}$ dependent for a three-dimensional (3D) system, apart from electron contribution $C_e(T) \sim \gamma T$ and phonon parts $C_{\text{ph}}(T) \sim \beta_1 T^3$ [1, 2]. In Co_3SnC , we first selected temperature ranges well above

the T_c for $11 \text{ K} \leq T \leq 15 \text{ K}$ ($C_M \sim 0$ at PM state). Thus, the plot of C_p/T vs T^2 is safely fitted by the formula $C_p/T = \gamma + \beta T^2$ at zero field as in the inset of Fig. 8(b), which gives $\gamma \sim 36.542(3) \text{ mJ/mol K}^2$ and $\beta \sim 0.130(1) \text{ mJ/mol K}^4$ for S1#. The γ value is an order larger than those of ordinary metals. Debye temperature Θ_D is calculated to be 421 K by the empirical formula $\Theta_D = 12\pi^4 NR/5\Theta_D^3$ ($N = 5$, and R is the gas constant). Using these parameters, the Wilson ratios $R_w = \pi^2 k_B^2 \chi/3\mu_B^2 \gamma$ (k_B is the Boltzmann constant, χ_s is the spin susceptibility, μ_B is the Bohr magneton) are about 19.6 (S1#) and 4.1 (S2#) if ignoring orbital contributions ($\chi_s = \chi_0$), which suggests strong electron-electron correlations in the ground state of Co_3SnC [37].

With increasing the field, logarithmic temperature divergence of $(C_p - C_{\text{ph}})/T$ is retained below 10 K in Fig. 8(b). As we know, the Schottky anomaly may usually cause similar temperature dependence of $C_p(T)$, which arises from energy splitting by fields [2, 38]. A low- T broad peak appears in the $C_p(T)$ for the Schottky anomaly and the $C_p(T)$ should increase with increasing the fields, but $(C_p - C_{\text{ph}})/T$ decreases monotonically for Co_3SnC , which excludes this possibility. Another interesting scenario is that NFL behavior rarely appears below and above the critical field in itinerant FM materials [2, 3, 39]. In most cases, this behavior can be understood based on magnetic clusters originating from competitions of the Ruderman-Kittel-Kasuya-Yosida (RKKY) coupling and the Kondo effect [3–6]. However, there is no evidence of RKKY interaction and the Kondo effect [22–24] and the present models are mainly constructed based on the localized magnetism near AFM QCPs [7]; thus reliable models are required to describe itinerant FM materials.

Furthermore, the field dependence of $(C_p - C_{\text{ph}})/T$ was calculated by subtracting the phonon contributions in Figs. 8(c) and 8(d) for several selected temperatures (2, 2.5, 3, 3.25, 3.5, 4, 4.5, 5, 5.5, and 6 K). At lower temperatures (for $T < T_c$, 2, 2.5, and 3 K), $(C_p - C_{\text{ph}})/T$ shows a slope change around H_a which can be defined as the intersections of two straight lines across the data as shown in Figs. 8(d) and S4 [32]; this slope change is mainly originated from different magnetic contributions and competitions. The H_a value increases gradually from ~ 0.30 T at 2 K to ~ 0.60 T at 3 K. However, at the elevated temperatures (for $T > T_c$, 3.25, 3.5, 4, 4.5, 5, 5.5, and 6 K), the field dependence of the $(C_p - C_{\text{ph}})/T$ exhibits a broad peak near H_a , which can be seen as the evidence for the endothermic process along with field-induced phase transition. However, the H_a value has different starting points owing to the ferromagnetic-paramagnetic phase transition although they show similar field dependence. Accordingly, we find that the H_a value shows a sharp jump at 3.25 K and increases from 0.10 T at 3.25 K to 1.20 T at 6 K. Therefore, the evolution of the H_a value with magnetic field may correlate with magnetic phase transition.

Figure 9(a) shows field dependence of $-d(C_p - C_{\text{ph}})/dT$ for Co_3SnC (S1#). Its value declines with increasing the field and is close to zero for $H > 4.0$ T. Using the linear extrapolation of $(C_p - C_{\text{ph}})/T$ to 1.0 and 1.8 K, the representative values γ_0 (1.0 K) and γ_0 (1.8 K) are gotten and field dependence of γ_0 (1.0 K) and γ_0 (1.8 K) are shown in Fig. 9(b); both show monotonic decrease with the

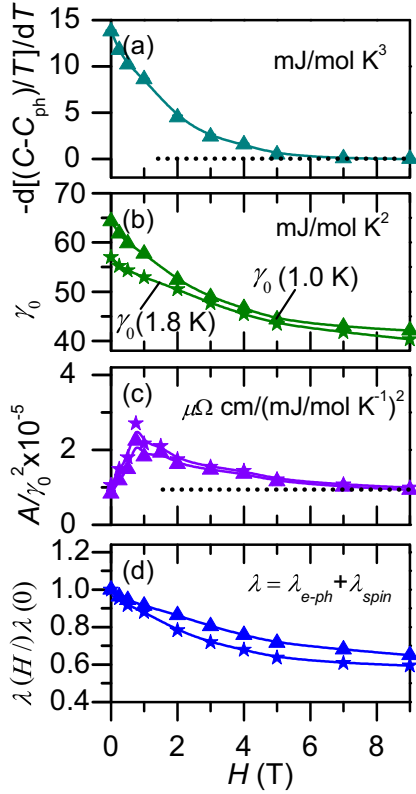


FIG. 9. Field dependence of the parameters: (a) the value of $-d(C_p - C_{ph})/T/dT$; (b) the γ_0 (1.0 K) and the γ_0 (1.8 K); (c) the A/γ_0^2 ; (d) the ratio $\lambda(H)/\lambda(0)$. The solid lines indicate the change tendency.

field. The field dependence of the Kadowaki-Woods ratio A/γ_0^2 is estimated in Fig. 9(c) [7]: It reaches a maximal value $\sim 3a_0$ [$a_0 = 10^{-5} \mu\Omega \text{ cm}/(\text{mJ}/\text{mol K})^2$] near H_c , and then decreases to $\sim a_0$ at 9.0 T. Large $A/\gamma_0^2 \sim 3a_0$ suggests the enhanced electron-electronic correlations and/or magnetic fluctuation and short characteristic length scales as expected in the itinerant spin-fluctuation theory [7], and the A/γ_0^2 value $\sim a_0$ at 9.0 T is consistent with the recovery of FL behavior [2]. In addition, the field-dependent evolution of the electron-electron interaction and magnetic fluctuation is roughly estimated. Usually, the formula $\gamma = \pi^2 k_B^2 N(E_F)(1 + \lambda)$ with the mass enhancement factor $\lambda = \lambda_{e-ph} + \lambda_{spin}$, where λ_{e-ph} represents the strengths of the electron-phonon coupling and λ_{spin} , can reflect the electron-electron interaction and magnetic fluctuations [2,38]. Given a fixed value of the density state at $N(E_F) \sim 3.99$ states/eV [25], the $\lambda(0)$ value is about $\sim 5-6$ and comparable to AlNi_3 (3.7 states/eV) [40] and ZrZn_2 (3.6 states/eV) [10]. The field dependence of the relative variations $\lambda(H)/\lambda(0)$ is estimated in Fig. 9(d). The $\lambda(H)/\lambda(0)$ decreases monotonically and reduces to $\sim 60\%$ at 9.0 T, which implies the gradual suppression of magnetic fluctuations and electron-electron correlations [2,38].

Figure 10(a) shows the temperature-field phase diagram of Co_3SnC (S1#). With increasing the field, the evolution of the characteristic parameter T_{FL} is shown. Below H_c , the T_{FL} is slightly reduced with increasing the fields and then increases gradually above H_c contrarily. In particular, above H_c , the T_{FL}

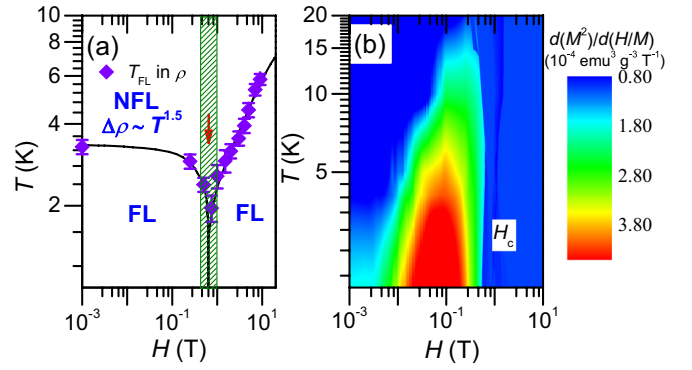


FIG. 10. Phase diagram and field dependence of the characteristic parameters for Co_3SnC (S1#): (a) the T_{FL} ; (b) the color shows its change tendency of $d(M^2)/d(H/M)$ vs H which is proportional to the magnitude of magnetic fluctuations.

is 3–4 K lower than the T_M value. It implies that NFL behavior persists for the temperature range $T_{FL} < T < T_M$ above H_c . For both, NFL behavior is retained up to 60 K, which indicates that the contributions from magnetic transition are not dominant, similar to the case of HF materials [3,4,11]. Thus, it is compelling to ascribe NFL behaviors to proximity to the field-induced magnetic instabilities in light of the phase diagram, although no single theory surely predicates all of the NFL behaviors [41]. As mentioned above, regarding the extremum of the derived parameters around the critical field, the origin is that the magnetic ground state can be manipulated by field, which can also affect the non-Fermi liquid and specific heat; however, its ground state may have complex nonlinear magnetic structures, which causes the characteristic parameters to show strong field dependence. This crossover can be closely correlated with the evolution of magnetic ground states under field, such as nonlinear to collinear ones, the subtle changes in the valence state of atoms, and field-induced suppression of some ordered phases as in Refs. [36,39]. Anyway, further studies may solve the remaining problems.

Finally, several important issues are proposed. As above, the NFL behavior in the itinerant FM state should be correlated with non-mean-field theory scaling. In itinerant FM material $\text{Sc}_{3,1}\text{In}$, the universality of QCP is described as magnetic fluctuations associated with the reduced crystallographic dimensionality [11]. In cubic Co_3SnC , the dimensionality is not concerned at all. A possible origin is the itinerant ferromagnetism with enhanced magnetic fluctuations near P_c for Co_3SnC . It is difficult to describe macroscopic magnetic fluctuations by susceptibility. As proposed in Ref. [42], the magnetic fluctuations can be estimated quantitatively by the isothermal magnetizations. In this model, the amplitude of the anisotropic magnetic fluctuations is assumed unchanged and the relative strength of magnetic fluctuations is proportional to the magnitude of $d(M^2)/d(H/M)$. Using this model and the $M(H)$ data in Fig. 6(d), magnetic fluctuations are roughly revealed and presented in Fig. 10(b). It is found that the enhanced magnetic fluctuations reach the maximum near P_c and the much smaller values above P_c are in conformity with the recovered FL behavior by the magnetic field. Moreover, lattice disorder and nonideal chemical

composition may be two other important factors to affect magnetism and electrical transport, especially for the excess Co atomic occupation in the corner site of cubic Co_3SnC which may result in more complicated magnetic interactions [22,24,33]. If so, the additional effect of the chemical component on the phase diagram needs further verification. It is also hoped that these results can promote the further study of micromagnetic detection technology and theoretical calculations.

IV. CONCLUSION

We report weak ferromagnetism and non-Fermi-liquid behavior of Co_3SnC . Under magnetic field, the exponent n in the temperature dependence of resistivity shows a crossover from $n = 1.0$ to 2.0. The coefficient of the T^2 term in resistivity shows $(H - H_c)^{-0.5}$ divergences at H_c and the mass enhancement factor $\lambda(H)/\lambda(0)$ reduces monotonically to $\sim 60\%$ at 9.0

T, indicating the gradual suppressions of magnetic fluctuation and electron-electron scattering.

ACKNOWLEDGMENTS

This work is supported by National Key Research and Development Program of China (Programs No. 2018YFA0305700 and No. 2018YFA0305800), Beijing Natural Science Foundation (Program No. Z190008), The Strategic Priority Research Program and Key Research Program of Frontier Sciences of the Chinese Academy of Sciences (Programs No. XDB25000000 and No. QYZDB-SSW-SLH013), the National Nature Science Foundation of China (Grants No. 11574377 and No. 51171177), IOP Hundred-Talent Program (Program No. Y7K5031X61), and Youth Promotion Association of CAS (Program No. 2018010).

-
- [1] P. Phillips, *Advanced Solid State Physics* (Cambridge University Press, Cambridge, 2008), p. 224.
- [2] G. R. Stewart, *Rev. Mod. Phys.* **73**, 797 (2001).
- [3] P. Gegenwart, J. Custers, C. Geibel, K. Neumaier, T. Tayama, K. Tenya, O. Trovarelli and F. Steglich, *Phys. Rev. Lett.* **89**, 056402 (2002); P. Gegenwart, J. Custers, Y. Tokiwa, C. Geibel, and F. Steglich, *ibid.* **94**, 076402 (2005).
- [4] E. D. Bauer, V. S. Zapf, P.-C. Ho, N. P. Butch, E. J. Freeman, C. Sirvent, and M. B. Maple, *Phys. Rev. Lett.* **94**, 046401 (2005).
- [5] H. V. Löhneysen, T. Pietrus, G. Portisch, H. G. Schlager, A. Schröder, M. Sieck, and T. Trappmann, *Phys. Rev. Lett.* **72**, 3262 (1994).
- [6] R. E. Baumbach, J. J. Hamlin, L. Shu, D. A. Zocco, J. R. O'Brien, P.-C. Ho, and M. B. Maple, *Phys. Rev. Lett.* **105**, 106403 (2010).
- [7] J. Custers, P. Gegenwart, H. Wilhelm, K. Neumaier, Y. Tokiwa, O. Trovarelli, C. Geibel, F. Steglich, C. Pépin, and P. Coleman, *Nature* **424**, 524 (2003).
- [8] K. Kuga, G. Morrison, L. R. Treadwell, J. Y. Chan, and S. Nakatsuji, *Phys. Rev. B* **86**, 224413 (2012).
- [9] K. Deguchi, S. Matsukawa, N. K. Sato, T. Hattori, K. Ishida, H. Takakura, and T. Ishimasa, *Nat. Mater.* **11**, 1013 (2012).
- [10] D. A. Sokolov, M. C. Aronson, W. Gannon, and Z. Fisk, *Phys. Rev. Lett.* **96**, 116404 (2006).
- [11] E. Svanidze, L. Liu, B. Frandsen, B. D. White, T. Besara, T. Goko, T. Medina, T. J. S. Munsie, G. M. Luke, D. Zheng, C. Q. Jin, T. Siegrist, M. B. Maple, Y. J. Uemura, and E. Morosan, *Phys. Rev. X* **5**, 011026 (2015).
- [12] E. Svanidze, T. Besara, J. K. Wang, D. Geiger, L. Prochaska, J. M. Santiago, J. W. Lynn, S. Paschen, T. Siegrist, and E. Morosan, *Phys. Rev. B* **95**, 220405(R) (2017).
- [13] P. M. Raccah and J. B. Goodenough, *Phys. Rev.* **155**, 932 (1967).
- [14] D. Fruchart and E. F. Bertaut, *J. Phys. Soc. Jpn.* **44**, 781 (1978).
- [15] F. Grandjean and A. Gérard, *J. Phys. F: Met. Phys.* **6**, 451 (1976).
- [16] T. He, Q. Huang, A. P. Ramirez, Y. Wang, K. A. Regan, N. Rogado, M. A. Hayward, M. K. Haas, J. S. Slusky, K. Inumara, H. W. Zandbergen, N. P. Ong, and R. J. Cava, *Nature* **411**, 54 (2001).
- [17] K. Takenaka and H. Takagi, *Appl. Phys. Lett.* **87**, 261902 (2005).
- [18] P. Tong, B. S. Wang, and Y. P. Sun, *Chin. Phys. B.* **22**, 067501 (2013).
- [19] S. Lin, P. Tong, B. S. Wang, J. C. Lin, Y. N. Huang, and Y. P. Sun, *Inorg. Chem.* **53**, 3709 (2014).
- [20] R. J. Huang, L. F. Li, F. S. Cai, X. D. Xu, and L. H. Qian, *Appl. Phys. Lett.* **93**, 081902 (2008).
- [21] X. G. Guo, J. C. Lin, P. Tong, M. Wang, Y. Wu, C. Yang, B. Song, S. Lin, W. H. Song, and Y. P. Sun, *Appl. Phys. Lett.* **107**, 202406 (2015).
- [22] L. Zhang, B. S. Wang, Y. P. Sun, P. Tong, J. Y. Fan, C. J. Zhang, L. Pi, and Y. H. Zhang, *Phys. Rev. B* **85**, 104419 (2012).
- [23] P. D. Babu and S. N. Kaul, *J. Phys.: Condens. Matter* **9**, 7189 (1997).
- [24] Y. B. Li, W. F. Li, W. J. Feng, Y. Q. Zhang, and Z. D. Zhang, *Phys. Rev. B* **72**, 024411 (2005).
- [25] D. F. Shao, W. J. Lu, P. Tong, S. Lin, J. C. Lin, and Y. P. Sun, *J. Phys. Soc. Jpn.* **83**, 054704 (2014).
- [26] C. Stoner, *Proc. R. Soc. London, Ser. A* **169**, 339 (1939).
- [27] T. Maruoka and R. O. Suzuki, *Mater. Trans.* **47**, 1422 (2006).
- [28] Y. Kimura, K. Sakai, F. G. Wei, and Y. Mishima, *Intermetallics* **14**, 1262 (2006).
- [29] M. Bilal, I. Ahmad, S. J. Asadabadi, R. Ahmad, and M. Maqbool, *Electron. Mater. Lett.* **11**, 466 (2015).
- [30] R. G. Greene, H. Luo, A. L. Ruoff, S. S. Trail, and F. J. DiSalvo, Jr., *Phys. Rev. Lett.* **73**, 2476 (1994).
- [31] J. Crain, G. J. Ackland, J. R. Maclean, R. O. Piltz, P. D. Hatton, and G. S. Pawley, *Phys. Rev. B* **50**, 13043(R) (1994).
- [32] See Supplemental Material at <http://link.aps.org/supplemental/10.1103/PhysRevB.102.085153> for the XRD resistivity, magnetic properties, and specific heat at of Co_3SnC .
- [33] L. H. Lewis, D. Yoder, A. R. Moodenbaugh, D. A. Fischer, and M.-H. Yu, *J. Phys.: Condens. Matter* **18**, 1677 (2006).

- [34] A. K. Pramanik and A. Banerjee, [Phys. Rev. B **79**, 214426 \(2009\)](#).
- [35] E. D. Mun, S. L. Bud'ko, C. Martin, H. Kim, M. A. Tanatar, J.-H. Park, T. Murphy, G. M. Schmiedeshoff, N. Dilley, R. Prozorov, and P. C. Canfield, [Phys. Rev. B **87**, 075120 \(2013\)](#).
- [36] N. P. Butch and M. B. Maple, [Phys. Rev. Lett **103**, 076404 \(2009\)](#).
- [37] A. C. Hewson, *The Kondo Problem to Heavy Fermions* (Cambridge University Press, Cambridge UK, 1993).
- [38] A. Tari, *The Specific Heat of Matter at Low Temperatures* (World Scientific, Hackensack, NJ, 2003), p. 250.
- [39] S. Ran, G. M. Schmiedeshoff, N. Pouse, I. Jeon, N. P. Butch, R. B. Adhikari, C. C. Almasan, and M. B. Maple, [Philos. Mag. **99**, 1751 \(2019\)](#).
- [40] P. Tong, Y. P. Sun, X. B. Zhu, and W. H. Song, [Phys. Rev. B **74**, 224416 \(2006\)](#).
- [41] D. Belitz, T. R. Kirkpatrick, M. T. Mercaldo, and S. L. Sessions, [Phys. Rev. B **63**, 174427 \(2001\)](#).
- [42] Y. Takahashi, [J. Phys.: Condens. Matter **13**, 6323 \(2001\)](#).